We are IntechOpen,
the world's leading publisher of
Open Access books
Built by scientists, for scientists

6,900
Open access books available

185,000
International authors and editors

200M
Downloads

Our authors are among the

154
Countries delivered to

TOP 1%
most cited scientists

12.2%
Contributors from top 500 universities

CLARIVATE ANALYTICS
BOOK CITATION INDEX
INDEXED

WEB OF SCIENCE™

Selection of our books indexed in the Book Citation Index
in Web of Science™ Core Collection (BKCI)

Interested in publishing with us?
Contact book.department@intechopen.com

1

Nuclear Excitation Processes in Astrophysical Plasmas

G. Gosselin[1], P. Mohr[2,3], V. Méot[1] and P. Morel[1]
[1]CEA,DAM,DIF, Arpajon
[2]Diakonie-Klinikum, Schwäbisch Hall
[3]ATOMKI, Debrecen
[1]France
[2]Germany
[3]Hungary

1. Introduction

In general, nuclear transitions are almost independent of the atomic environment of the nucleus. This feature is a basic prerequisite for the widely used nuclear chronometers (with the most famous example of ^{14}C, the so-called radiocarbon dating). However, a closer look at the details of nuclear transitions shows that under special circumstances the atomic environment may affect nuclear transitions. This is most obvious for electron capture decays where the nucleus captures an electron (typically from the lowest K-shell). A nice example for the experimental verification of this effect is the dependence of the electron capture half-life of [7]Be on the chemical form of the beryllium sample (Ohtsuki et al., 2004). Also the half-lives of β--decays may be affected by the environment: for fully ionized nuclei the emitted electron may remain in the (otherwise completely occupied) K-shell, thus enhancing the decay Q-value and decay rate. An experimental verification was found for [187]Re (Bosch et al., 1996). As electron densities in solids may also vary with temperature (e.g. in the Debye-Hückel model), β-decay half-lives may also depend on temperature. However, the latest study of the decay branching between β--decay and β+-decay/electron capture in [74]As could not confirm earlier claims in this direction (Farkas et al., 2009). The relevance of temperature and density dependence of β-decay has been studied in detail in the review (Takahashi and Yokoi, 1987).

Contrary to the above mentioned β-decays where the role of electrons in the environment of the nucleus is obvious, the present study investigates electromagnetic transitions in nuclei. We also do not analyze electron screening where stellar reaction rates between charged particles at extremely low energies are enhanced because the repulsive Coulomb force between the positively charged nuclei is screened by the electrons in the stellar plasma. Details on electron screening can also be found in this book (Kücük, 2012) and in the latest review of solar fusion reactions (Adelberger et al., 2011).

The electromagnetic transitions under study in this chapter are extremely important in almost any astrophysical scenario. Capture reactions like (p,γ), (n,γ), and (α,γ) play key roles

in hydrostatic and explosive burning of stars, in the neutrino production of our sun, and in the synthesis of heavy elements in the so-called s-process and r-process. Photodisintegration reactions like (γ,p), (γ,n) and (γ,α) define the reaction path in the so-called γ-process which produces a significant amount of the rare p-nuclei. In addition, half-lives of isomeric states may be affected under stellar conditions via photon-induced excitation of so-called intermediate states.

As we will show in this chapter, γ-transitions which are most affected by the electronic environment are found in heavy nuclei and are characterized by relatively low γ-transition energies below approximately 100 keV. First of all, astrophysical processes have to be identified where such γ-transitions play an important role.

In early burning stages of stars from hydrogen burning up to silicon burning heavier nuclei are synthesized mainly by capture reactions along the valley of stability. Typical Q-values of these capture reactions between light nuclei are of the order of several MeV. In these scenarios γ-transitions are practically not affected by the surrounding plasma. A possible exception in the $^7Be(p,\gamma)^8B$ reaction will be discussed separately as a special example later in this chapter.

The synthesis of heavy nuclei proceeds mainly via neutron capture reactions in the slow and rapid neutron capture processes (s-process, r-process). The s-process path is located close to stability, and typical Q-values for neutron capture reactions are again of the order of several MeV. The corresponding capture γ-rays are also not significantly affected by the environment. As the r-process operates close to the neutron dripline, typical Q-values decrease down to about 2-3 MeV or even below. However, under typical r-process conditions an equilibrium between the (n,γ) capture and (γ,n) photodisintegration reaction is found, and the r-process path becomes mainly sensitive to the neutron separation energies, but almost independent of the corresponding (n,γ) and (γ,n) cross sections. Although there may be some influence of the plasma environment on the low-energy γ-transitions in the r-process, there is no significant influence on the outcome of the r-process.

Contrary to the s-process and the r-process, the so-called rp-process proceeds via proton captures on the neutron-deficient side of the chart of nuclides close to the proton dripline. The Q-values of these (p,γ) reactions may become small. However, in general not much is known on nuclei on the path of the rp-process, and thus any discussion of the influence of the surrounding plasma on low-energy γ-transitions in the rp-process must remain quite speculative and is omitted in this chapter.

In the so-called p-process or γ-process existing heavy seed nuclei are destroyed in the thermal photon bath of a hot environment by (γ,p), (γ,n) and (γ,α) reactions leading to the production of the low-abundance p-nuclei. Again, the required γ-ray energy is of the order of several MeV, by far too high for a significant influence of the plasma environment.

Further details on the various nucleosynthesis processes can be found in the latest textbooks (Iliadis, 2007; Rolfs and Rodney, 1988) and in several contributions to this book (Matteucci, 2012; Pumo, 2012; Arnould and Goriely, 2012).

At first view, it seems that the plasma environment is not able to play a significant role in any of the above processes. However, a closer look at the s-process nucleosynthesis shows that there are a number of cases where low-energy γ-transitions turn out to be extremely

important because such transitions may be able to produce and/or destroy isomers and thus affect s-process nucleosynthesis. The s-process path is located along the valley of stability. The level schemes of the nuclei under study are well-known; this holds in particular for the excitation energies and spins. This information allows for a careful study of the influence of the plasma.

Details of the s-process are given in this book (Pumo, 2012) and in a recent review (Käppeler et al., 2011). Here we repeat very briefly the most important properties of s-process nucleosynthesis. The main component of the s-process operates in low-mass AGB stars. Two alternating neutron sources are active. The $^{13}C(\alpha,n)^{16}O$ reaction operates for about 10^4 to 10^5 years at low temperatures below 10 keV; in most cases this temperature is too low to affect isomer production or destruction. The $^{22}Ne(\alpha,n)^{25}Mg$ reaction is activated for a few years during so-called helium shell flashes at temperatures around 25 keV and densities of about 10^3 g/cm³. (Gallino et al., 1998). Under these conditions dramatic variations of isomer production and destruction rates can be expected (Ward & Fowler, 1980; Mohr et al. 2007; Gintautas et al., 2009; Mohr et al., 2009; Hayakawa et al., 2010). It has to be noted that the stellar transition rates may exceed the experimentally accessible ground state contribution (Belic et al., 2002; Mohr et al., 2007b; Rauscher et al., 2011) by orders of magnitude.

Two different temperature dependencies can be found for such low-energy γ-transitions which should not be mixed up. First, the total transition rate between states is given by the sum over all contributing branchings; all these different contributions vary strongly with temperature because of the exponential temperature dependence of the surrounding blackbody radiation. Second, each individual transition may additionally be modified by the plasma environment; this may lead to an additional temperature and density dependence of individual transitions with low γ-ray energy. The latter effect is the main subject of this chapter.

As example we have chosen the nucleus ^{171}Tm. It has a ground state with $J^\pi = 1/2^+$ and a low-lying first excited state with $J^\pi = 3/2^+$ at the excitation energy of 5.04 keV. This state decays by a M1 transition with small E2 admixture (mixing $\delta = 0.021\pm0.001$) with a half-life of $T_{1/2} = 4.77\pm0.08$ ns. Because of its low energy, this transition is highly converted (internal conversion coefficient $\alpha = 1408\pm55$). All data have been taken from the latest data evaluation (Baglin, 2002). ^{171}Tm is located on a neutron-rich branch of the s-process and may be reached either via the branching at ^{169}Er in the $^{168}Er(n,\gamma)^{169}Er(n,\gamma)$ $^{170}Er(n,\gamma)$ $^{171}Er(\beta^-)^{171}$Tm reaction chain or via the branching at ^{170}Tm in the $^{169}Tm(n,\gamma)^{170}Tm(n,\gamma)^{171}$Tm chain. It is interesting to note that the destruction of ^{171}Tm in the $^{171}Tm(n,\gamma)^{172}$Tm capture reaction proceeds mainly via neutron capture in the thermally excited $3/2^+$ state (Rauscher et al., 2011).

2. Modification of a particular transition

As mentioned above, nuclear excitation in astrophysical plasmas may be significantly modified by the electronic environment γ-transitions of relatively low energy. Particles from the plasma other than photons interact with the nucleus and may excite it to an upper level. Thermodynamic conditions in the plasma may substantially alter the electronic environment of the nucleus and also perturb the de-excitation process of internal conversion. As a rule of thumb, every transition with an energy lower than 100 keV must be looked at, as internal

conversion can significantly contribute to the transition rate. Some examples for several γ-transition energies have already been shown earlier (Gosselin et al., 2010). The two levels involved need not include the ground state, but can also be built on an isomeric state.

At least four different electromagnetic excitation processes may be able to excite a nucleus under typical astrophysical plasma conditions (Gosselin et al., 2010):

- Radiative excitation. A photon from the blackbody spectrum in the plasma is absorbed by the nucleus (Ward & Fowler, 1980).
- Nuclear Excitation by Electron Capture (NEEC). A free electron from the plasma is captured onto an empty atomic shell, giving its energy to the nucleus. This is also known as Inverse Internal Conversion (Gosselin & Morel, 2004).
- Nuclear Excitation by Electron Transition (NEET). A loosely bound electron makes a transition to a deeper atomic shell and gives its energy to the nucleus (Morel et al., 2004).
- Inelastic scattering of electrons (Gosselin et al., 2009).

Another non-electromagnetic excitation process is inelastic neutron scattering. It will not be dealt with in here, as it is strongly dependent on the specific astrophysical plasma in which it occurs. As the neutron spectrum is not directly related to the thermodynamic conditions of the plasma, but rather to the astrophysical site under study, it is impossible to plot an excitation rate as a function of the temperature as for the other processes.

All these electromagnetic processes must be dealt with along with their inverse processes, respectively photon emission, internal conversion, bound internal conversion (BIC), super-elastic scattering of electrons (a scattering process where the scattered electron gains some energy from the nucleus) and neutrons.

Describing each process is a two-step undertaking. The first step is a microscopic description of the excitation process which uses quantum mechanics formalism and aims at calculating a cross section (when there is an incident particle) or a transition rate (when there is none, such as with NEET). The electronic environment of the nucleus is described with a relativistic average atom model (RAAM) (Rozsnyai, 1972) from which an atomic potential can be extracted which depends on the density and the temperature of the plasma.

The second step is to derive a macroscopic plasma transition rate for all processes. Thermodynamics and plasma physics in the RAAM model are used to get distribution functions of photons or electrons and build the corresponding transition rate. Except for NEET, such a model is able to provide reliable values of electronic shells binding energies and occupancies, as well as a distribution function of free electrons.

If the plasma can be considered to be at local thermodynamic equilibrium (LTE), the excitation and de-excitation rate of each process are related to each other by:

$$\frac{\lambda_e}{\lambda_d} = \frac{2J_f + 1}{2J_i + 1} e^{-\frac{\Delta E}{kT}}$$

(1)

In this expression, λ_e is the excitation rate, λ_d the de-excitation rate, J_i and J_f the spins of the initial and final states in the nucleus and ΔE the nuclear transition energy. This relation is known as the principle of detailed balance and expresses the micro-reversibility of excitation

processes. Here, we consider that electrons and photons are at LTE, but obviously nuclei are not.

2.1 Radiative excitation

Radiative excitation occurs through the resonant absorption of a photon. Most astrophysical plasmas have a large blackbody component in their photon spectrum. A blackbody photon can easily be absorbed by a nucleus if its energy is very close to a nuclear transition energy. However, the huge number of blackbody photons ensures that the resulting rate is significant. Two de-excitation processes compete with photon absorption: spontaneous and induced emission.

The microscopic cross section is a Breit and Wigner resonant capture cross section (Hamilton, 1975):

$$\sigma(h\nu) = \frac{2J_f + 1}{2(2J_i + 1)} \pi \hbar^2 c^2 \frac{\Gamma_\gamma \Gamma}{(h\nu)^2 \left[(h\nu - \Delta E)^2 + \frac{\Gamma^2}{4} \right]} \tag{2}$$

Here ν is the photon frequency, Γ_γ the gamma width of the excited nuclear level and Γ its total width. By folding this cross section with the blackbody distribution, we deduce an excitation rate:

$$\lambda_e = \frac{2J_f + 1}{2J_i + 1} \frac{\ln 2}{T_{J_f \to J_i}^\gamma} \frac{1}{e^{\frac{\Delta E}{kT_r}} - 1} \tag{3}$$

where T_r is the radiative temperature and $T_{J_f \to J_i}^\gamma$ the transition radiative half-life.

The induced de-excitation rate can be deduced from the spontaneous rate by multiplying by the number of modes:

$$\lambda_d^{ind} = n_\nu \lambda_d^{sp} = \frac{c^2 I_\nu}{2h\nu^3} \frac{\ln 2}{T_{J_f \to J_i}^\gamma} \tag{4}$$

where I_ν is the blackbody radiative intensity. This gives a total de-excitation rate:

$$\lambda_d = \frac{\ln 2}{T_{J_f \to J_i}^\gamma} \frac{e^{\frac{\Delta E}{kT_r}}}{e^{\frac{\Delta E}{kT_r}} - 1} \tag{5}$$

This total de-excitation rate and the excitation rate satisfy the principle of detailed balance.

As mentioned above, all excitation processes were calculated for [171]Tm. Fig. 1 shows excitation and induced emission rates becoming significant when the plasma temperature reaches a value in the same order of magnitude as the nuclear transition energy.
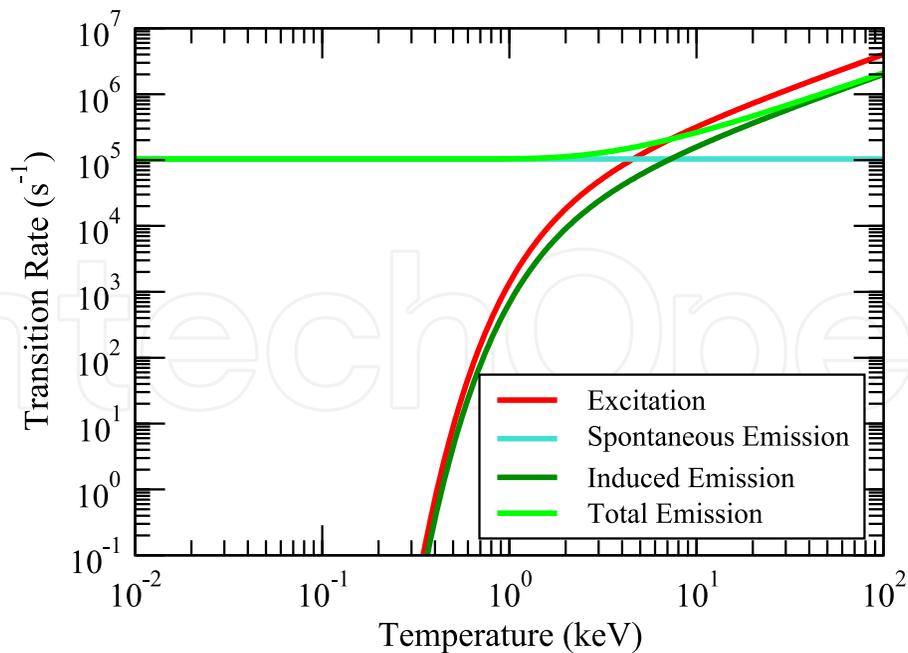
Fig. 1. Radiative excitation and de-excitation of ^{171}Tm.

2.2 Nuclear excitation by electron capture

NEEC is the inverse process of internal conversion. A free electron from the plasma is captured onto an atomic shell and the excess energy is used to excite the nucleus. It still has not been observed in the laboratory despite some attempts in channeling experiments (Kimball et al., 1991) and some projects with EBIT or EBIS (Marss, 2010). Considering NEEC in plasmas has first been proposed by Doolen (Doolen, 1978) in plasma at LTE.

If an electron has a kinetic energy lower than the nuclear excitation energy, the NEEC cross section can be expressed by the Fermi golden rule (Messiah, 1961):

$$\sigma_{NEEC}(E) = \frac{2\pi}{\hbar v_e} \left| \left\langle \psi_f \varphi_b \left| H \right| \psi_i \varphi_r \right\rangle \right|^2 \rho_b(E) \tag{6}$$

where v_e is the incident electron speed, Ψ_i and Ψ_f the nuclear initial and final states wave functions, φ_b and φ_r the bound and free electron wave functions and $\rho_b(E)$ the total final state density. The matrix element is directly related to the internal conversion coefficient (Hamilton, 1975), which gives a resonant electron capture cross section:

$$\sigma_{NEEC}(E) = \frac{\pi\hbar^2}{2m_eE} \frac{2J_f+1}{2J_i+1} \frac{\ln 2}{T^{\gamma}_{J_f \to J_i}} \alpha \frac{\hbar\Gamma}{\left(E-E_r\right)^2 + \left(\frac{\Gamma}{2}\right)^2} \tag{7}$$

where $T^{\gamma}_{J_f \to J_i}$ is the radiative half-life of the transition, α the internal conversion coefficient, E_r the resonance energy and Γ the nuclear level width.

A NEEC rate in plasma can then be derived by folding this cross section with the free electron distribution:

$$\lambda_e = \frac{2J_f+1}{2J_i+1}\frac{\ln 2}{T^{\gamma}_{J_f \to J_i}}\alpha(T_e)f_{FD}(E_r)\big[1-f_{FD}(E_b)\big] \tag{8}$$

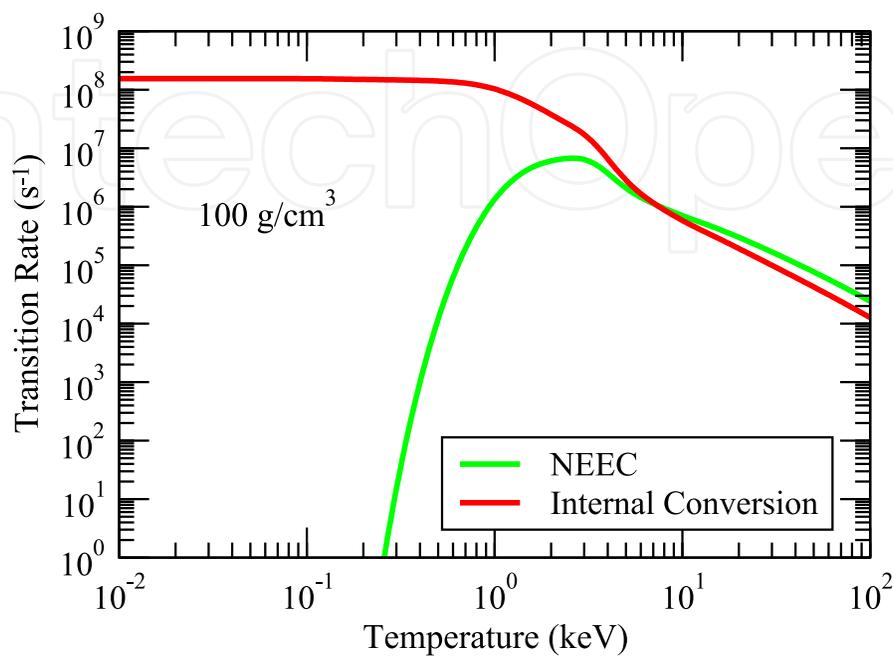with E_b the binding energy of the bound electron and f_{FD} is the Fermi-Dirac distribution.

Fig. 2. NEEC excitation and Internal Conversion de-excitation of [171]Tm.

At low temperatures, Fig. 2 shows a near constant internal conversion rate which is very close to the laboratory value. For higher temperatures, the number of bound electrons decreases as the atom is ionized, and the number of allowed conversions must decrease. At low temperatures, the NEEC rate is very small as there are few free electrons to be captured and few vacant atomic states on which they could be captured. The NEEC rate then rises as the temperature increases to reach a maximum. The decrease at the higher temperatures can be attributed to the rising kinetic energy of the free electrons, the fraction of which below the nuclear transition threshold becoming less and less important.

2.3 Nuclear excitation by electron transition

Nuclear Excitation by Electron Transition (NEET) occurs when a loosely bound electron makes a transition to a deeper atomic shell and gives its energy to the nucleus. This may happen when the electronic and nuclear transition energies are very close to each other (separated by less than the atomic widths). NEET requires at least one electron on the outer atomic shell and at least a vacancy on the inner atomic shell. The energy difference between the atomic and the nuclear transition energy is called the mismatch and is denoted by δ. In the laboratory, such restrictive conditions can only be achieved for a very small number of nuclei. In astrophysical plasma, various conditions of density and temperature can be encountered, with a huge number of different electronic configurations at various charge states. The electronic shell binding energies are modified and the energy resonance condition (δ≈0) can more often be achieved.

The probability of NEET occurring on an isolated and excited atom is given by:

$$P_{NEET}(\delta) = \frac{|R_{1,2}|^2}{\delta^2 + \left(\dfrac{\Gamma_1 + \Gamma_2}{2}\right)^2}\left(1 + \frac{\Gamma_2}{\Gamma_1}\right) \tag{9}$$

where Γ_1 and Γ_2 represent the total width (atomic and nuclear) of the initial and final configurations, respectively, and $|R_{1,2}|$ is the atom-nucleus matrix coupling element (Morel et al., 2004). The NEET probability reaches a maximum when the mismatch is zero. Mismatch variations for a 3s-6s atomic transition on Fig. 3 exhibit matching conditions around a temperature of 4 keV for a plasma density of 100 g/cm³.
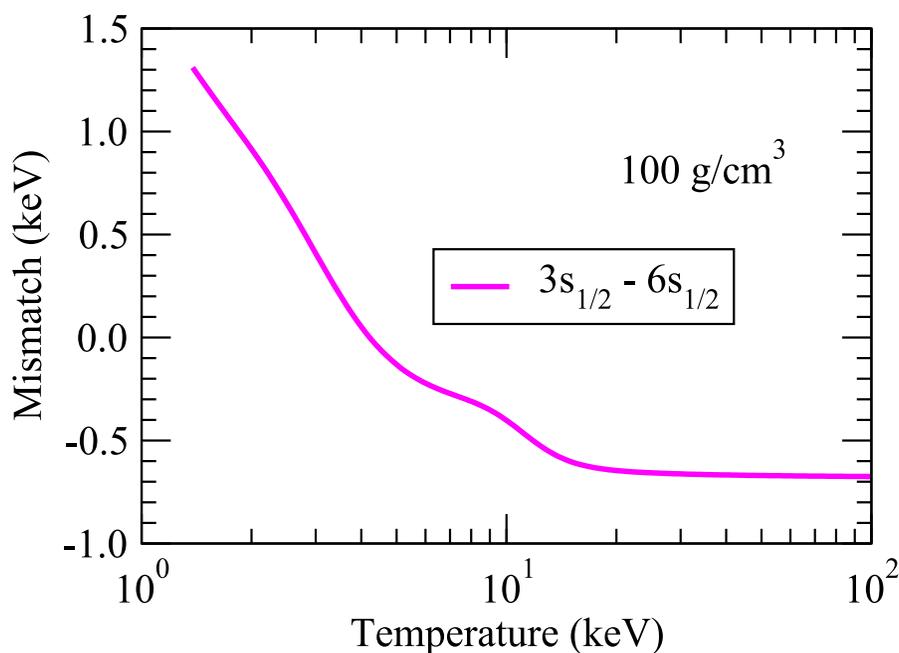
Fig. 3. Mismatch of ($3s_{1/}$ –$6s_{1/2}$) atomic transition for [171]Tm.

The atom-nucleus coupling matrix element is little sensitive to temperature as illustrated on Fig. 4. As the temperature increases, there are less bound electrons. This reduces screening of the nucleus by the remaining bound electrons, whose orbitals are closer to the nucleus. The overlap between the electron and the nucleus wave functions is larger, which increases the coupling.

In plasma, the NEET rate can be estimated as a summation over all initial configurations of the rate of creation of such a configuration multiplied by the NEET probability:

$$\lambda^{NEET}(\rho, T_e) = \sum_\alpha P_\alpha(\rho, T_e)\frac{\Gamma_\alpha}{\hbar}N_1\left(1 - \frac{N_2}{\Omega_2}\right)\frac{|R_{\alpha,\beta}|^2}{\delta_{\alpha,\beta}^2 + \left(\dfrac{\Gamma_\alpha + \Gamma_\beta}{2}\right)^2} \tag{10}$$

Here, N_1 and N_2 are the initial electronic occupations of the two atomic shells involved in the transition, of degeneracy Ω_1 and Ω_2, corresponding to outer and inner shell, respectively.
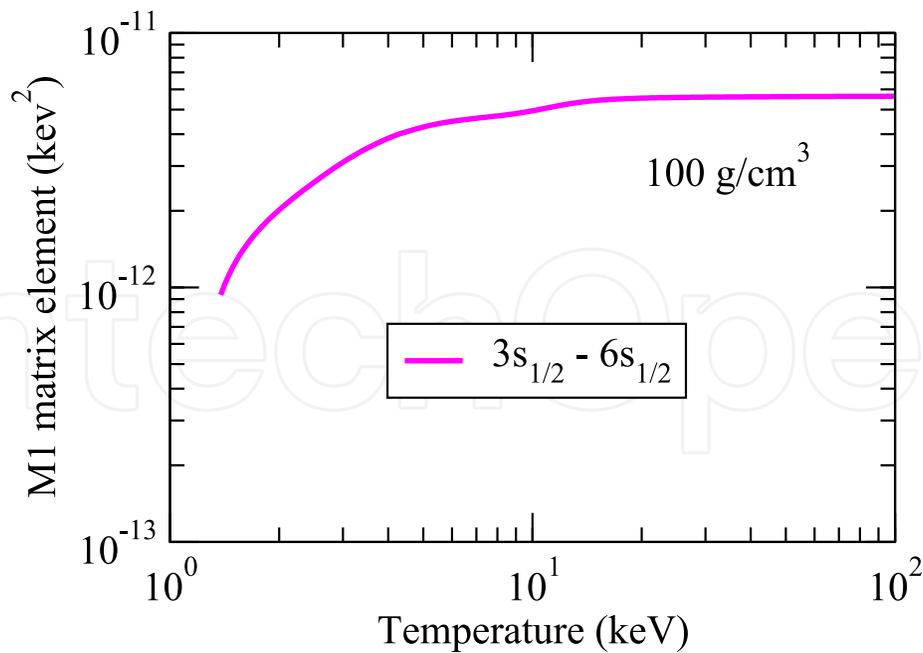
Fig. 4. Atom-Nucleus coupling matrix element of ($3s_{1/2}$–$6s_{1/2}$) atomic transition for ^{171}Tm.

An accurate calculation requires a good knowledge of nuclear and atomic wave functions for every configuration. However, the huge number of electronic configurations in this approach, which mirrors the DCA (Detailed Configuration Accounting) approach used to determine atomic spectra (Abdallah et al., 2008), makes such a calculation a prohibitive task. Therefore, we replace the detailed spectrum of atomic transitions by a Gaussian envelope, whose mean energy and statistical standard deviation σ are extracted from the RAAM (Faussurier et al., 1997). This quicker approach works the best when only outer atomic shells are involved. The NEET rate becomes:

$$\lambda^{NEET}\left(\rho,T_e\right) = \frac{2\pi}{\hbar}N_1\left(1-\frac{N_2}{\Omega_2}\right)\left|R_{1,2}\right|^2\frac{1}{\sqrt{2\pi\sigma^2}}e^{-\frac{\delta^2}{2\sigma^2}} \tag{11}$$

The NEET rate as a function of electronic temperature is presented in Fig. 5. Many atomic transitions contribute to the total NEET rate, the $3s_{1/2}$–$6s_{1/2}$ and $3p_{1/2}$-$6p_{3/2}$ transitions being the two dominant ones around 4 keV (only the M1 and E2 transitions with a maximum NEET rate higher than 10^3 s^{-1} are shown).

The average atom model cannot be steadily applied for atomic transitions involving deep shells because their average occupation numbers differ highly from the NEET requirements of at least a vacancy in the inner shell and an electron in the outer shell. In such cases, the mismatch of the RAAM mean configuration can be very different from the mismatches of the real configurations on which NEET is possible. When this discrepancy gets higher than the statistical standard deviation, a detailed configuration approach such as DCA can then not be avoided.

Fully comprehensive DCA calculations are still out of reach of the fastest available supercomputers. However, a careful selection of the atomic transitions may significantly reduce the number of electronic configurations and may soon be an accessible goal.
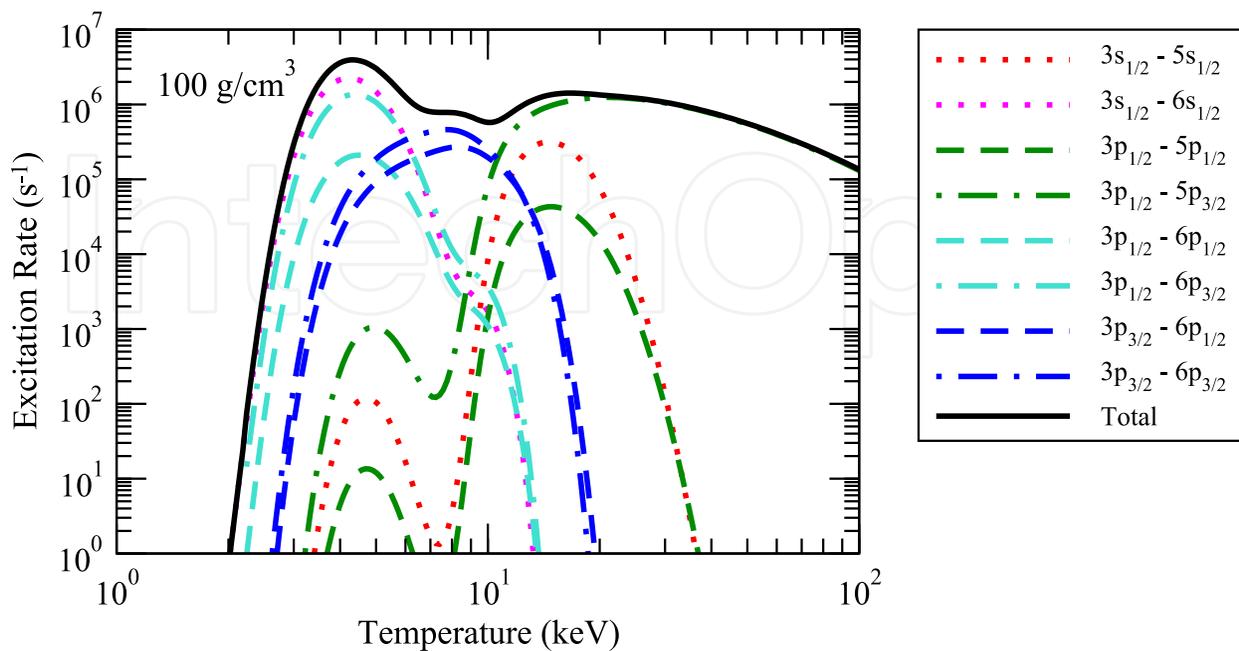
Fig. 5. NEET excitation of [171]Tm.

2.4 Inelastic electron scattering

In astrophysical plasmas, there usually exists a huge number of free electrons. If the nuclear transition energy is low enough, a significant part of these electrons might be able to excite the nucleus through Coulomb excitation. A semi-classical theory works well for high -above 1 MeV- energy ions (Alder et al., 1956), whereas a more sophisticated quantum model is required to deal with electrons in the keV range. With an unscreened atomic potential, a WKB approximation can be successfully implemented (Gosselin et al., 2009). The WKB cross section is very close to the more exact usual DWBA quantum approach (Alder et al., 1956) but much computationally heavier.

Cross sections exhibit usually low values in the 10^{-30} cm^2 range which can be at least partially compensated by the huge number of free electrons in high temperature plasmas (above the nuclear transition energy). However, these cross sections also exhibit a non-physical behavior close to the energy threshold where it does not drop to zero as it should do, as can be seen on Fig. 6. This can be explained by an "acceleration" of the incident electron by the unscreened potential as the global neutrality of the atom is not verified. Using a screened potential in the future will allow to get rid of this artifact.

By folding this cross section with the free electron distribution, we easily deduce an electron inelastic scattering excitation rate in plasma as shown on Fig. 7. It is negligible at low temperatures when there are very few free electrons, and these electrons do not have a high enough energy to be above the threshold. This changes when the temperature reaches values around the nuclear transition energy. At high temperatures, the excitation rate does not vary much as the lowering cross section is compensated by the increasing velocity of the electrons.
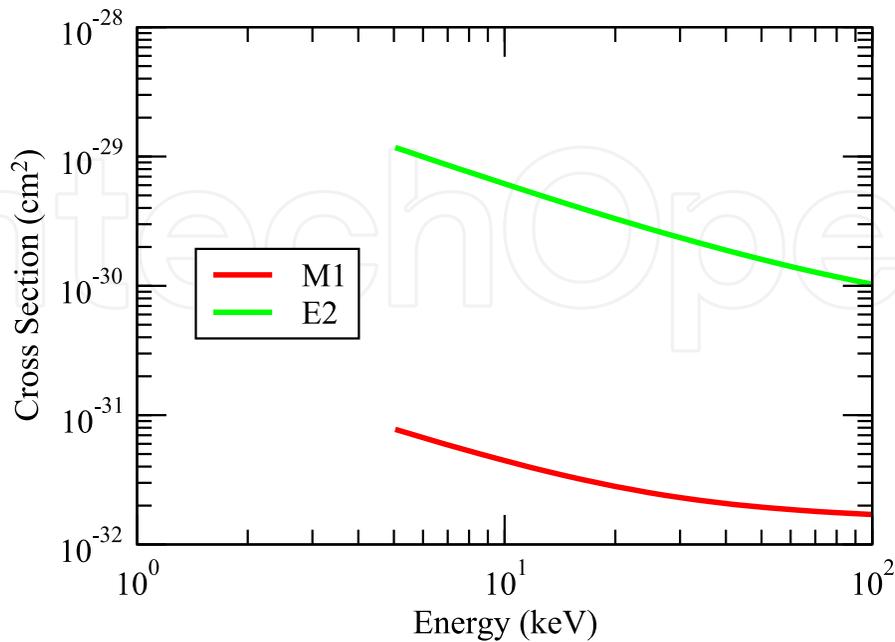
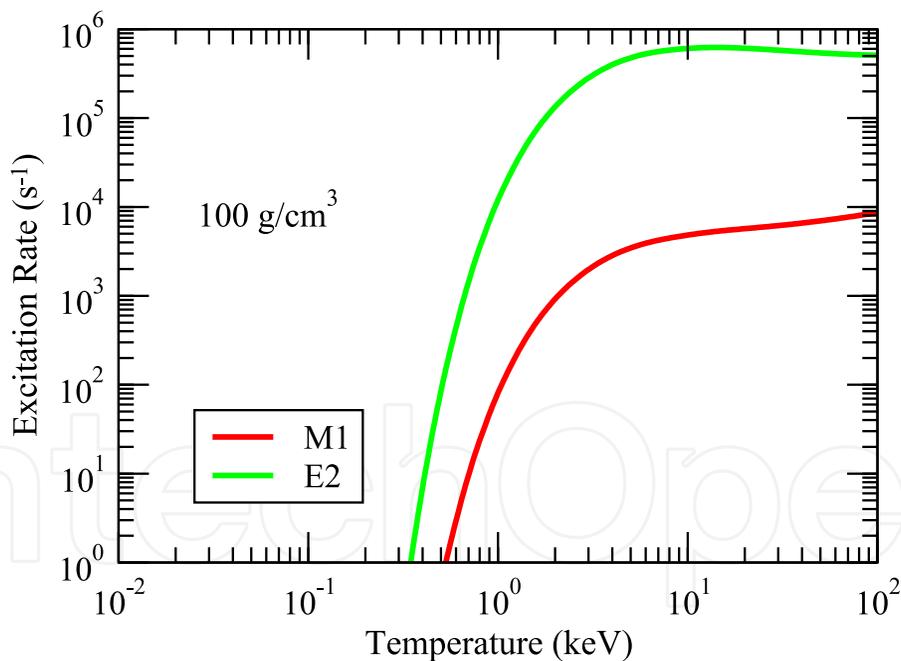Fig. 6. WKB Inelastic electron scattering cross section of ^{171}Tm.

Fig. 7. Inelastic electron scattering excitation rate of ^{171}Tm.

2.5 Lifetime evolution

Fig. 8 summarizes excitation rates of the four electromagnetic processes present in plasma. NEEC dominates at low temperatures, radiative excitation at the hottest temperatures and NEET in between. The electron inelastic scattering never dominates although this situation could change at higher plasma density.
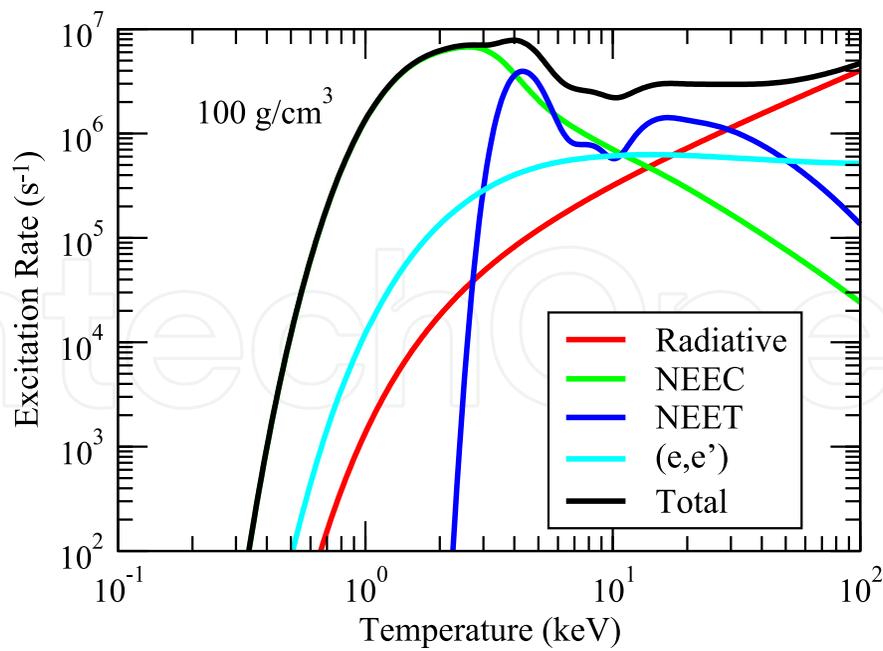
Fig. 8. Nuclear excitation rate in plasma of [171]Tm.

Highly variable rates of excitation also means highly variable rates of de-excitation which means that the nuclear lifetime of the excited level now depends on the plasma temperature. Fig. 9 shows these variations which cover nearly two orders of magnitude in the particular example of [171]Tm at 100 g/cm^{3}. Some other nuclei even exhibit larger variations, such as [201]Hg (Gosselin et al., 2007) where the lifetime can be increased by a factor of more than 10[4].
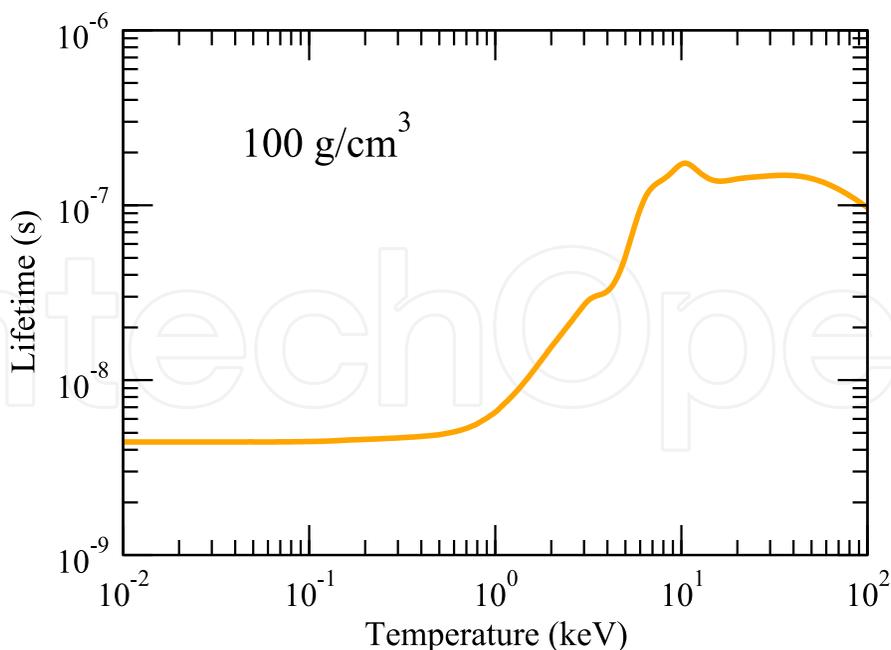

Fig. 9. Lifetime in plasma of [171]Tm.

However, this lifetime is an extension of the usual notion of lifetime in the laboratory. This plasma lifetime is the characteristic time required to get from any relative populations of

both the ground and excited states to the LTE (for the nuclear levels) relative populations, that is populations whose ratio is given by the Boltzmann factor. For high temperatures and a higher spin for the excited state, the population of the excited state reaches a higher value than that of the ground state.

3. Stellar transition rates

As shown before in this chapter, thermalization between the ground state and the first excited state of ^{171}Tm is achieved on a timescale far below 1 second, i.e. much faster than the timescales of the astrophysical s-process. This result remains valid as long as the levels under study are connected by a direct γ-transition or a γ-cascade. A similar result has been derived explicitly for the ground state band of ^{176}Lu (Gintautas et al., 2009). Thus, because of the prompt thermalization within γ-bands it is obvious that the stellar transition rate of any photon-induced reaction has to be calculated including all contributions of thermally excited states. This holds in particular for (γ,n) and (γ,α) reactions for the astrophysical γ-process, but also for the photodestruction of isomers in the s-process. Because the required photon energies for (γ,n) and (γ,α) reactions is of the order of several MeV, the influence of the surrounding plasma remains small, and we focus on the photodestruction of isomers in the following.

The *K*-isomers are found in heavy deformed nuclei. Transitions between states with large differences in the *K* quantum number are strongly suppressed by selection rules. Thus, there are no direct transitions between low-*K* states and high-*K* states. As a consequence, thermalization has to proceed via higher-lying so-called intermediate states (IMS) with intermediate *K* quantum number which have a decay branching to the low-*K* and to the high-*K* part of the excitation spectrum of the respective nucleus. The transition rates from the low-*K* side and the high-*K* side of the spectrum to the IMS define the timescale for thermalization. Typically, these IMS are located at excitation energies above 500 keV. They decay down to the lowest states with low and high *K* by γ-cascades where energies of the individual γ-transitions are obviously much smaller than the excitation energy, i.e. the energies may be as low as 100 keV or even below. This is the energy region where the plasma effects become important. The full formalism for the calculation of stellar reaction rates is given in an earlier work (Gosselin et al., 2010). The essential result is that the stellar reaction rate λ^* for transitions from the low-*K* to the high-*K* states (and reverse) can be derived by a formula similar to Eq. (2) which leads to

$$\lambda^* \propto \frac{\Gamma_1 \Gamma_2}{\Gamma_1 + \Gamma_2} \tag{12}$$

where Γ_1 and Γ_2 are the total decay widths to the low-*K* and the high-*K* states respectively in the deformed nucleus under stellar conditions (i.e., summed over all levels, each particular transition width $\Gamma_{i \to f}$ being modified by the plasma environment according to the discussion in this work). It should be noted that the smaller of the two widths Γ_1 and Γ_2 essentially defines the stellar reaction rate λ^* for transitions from the low-*K* to the high-*K* states because the larger width cancels out in the above equation.

4. Some selected examples

In the following section we discuss three examples in greater detail. The first two examples are so-called *K*-isomers which are relevant in the astrophysical s-process (^{176}Lu and ^{180}Ta). The last example is the ^{7}Be(p,γ)^{8}B reaction with its low reaction Q-value of 137 keV.

4.1 ^{176}Lu in the astrophysical s-process

^{176}Lu is a so-called s-only nucleus because it is synthesized only in the astrophysical s-process. It is produced either in its high-*K* *J*^{π};*K*=7^{-};7 ground state with a half-life of 38 giga-years (quasi-stable for the s-process) or in its low-lying low-*K* *J*^{π};*K*=1^{-};0 isomer at 123 keV with a half-life of less than 4 hours. The ^{175}Lu(n,γ)^{176}Lu reaction produces most of ^{176}Lu in the low-*K* isomeric state which decays by β^{-} emission to ^{176}Hf. ^{176}Lu can only survive if the isomer is coupled to the high-*K* ground state (Heil et al., 2008). The most relevant IMS for this coupling is located at 839 keV with *J*^{π};*K*=5^{-};4, although other IMS have been suggested very recently (Gintautas et al., 2009; Dracoulis et al., 2010).

The IMS at 839 keV decays predominantly to the high-*K* part of ^{176}Lu; thus, the decay branch to the low-*K* part defines the stellar reaction rate. The decay properties of the IMS at 839 keV are well known from various γ-spectroscopic studies (Doll et al., 1999; Klay et al., 1991; Lesko et al., 1991). The lowest γ-ray energy is 123 keV, and three further γ-rays are observed at higher energies. Because of the relatively high energies the stellar reaction rate is only weakly affected. The dominating effect is NEEC in this case. However, the modification of the stellar transition rate remains far below a factor of two in the astrophysically relevant energy region (Gosselin et al., 2010).

4.2 ^{180}Ta and its uncertain nucleosynthetic origin

^{180}Ta is the rarest nucleus in our solar system (Lodders, 2003), and it is the only nucleus which does not exist in its ground state, but in an isomeric state. The ground state is a low-*K* state with *J*^{π};*K*=1^{+};1 and a short half-life of 8.154 hours. The isomer is located at an excitation energy of 77 keV; it is a high-*K* state with *J*^{π};*K*=9^{-};9. Because of its huge *K* quantum number, its decay to the ground state is highly suppressed, and also the energetically possible β-decays to ^{180}Hf and ^{180}W are largely hindered. The half-life of the isomer is unknown with a lower limit of 7.1 x 10^{15} years (Hult et al, 2006; Wu & Niu, 2003). Despite significant effort, the nucleosynthetic origin of ^{180}Ta is still uncertain.

Various astrophysical sites and corresponding processes have been suggested for the nucleosynthesis of ^{180}Ta. Very recently it has been concluded that a large contribution to the solar abundance can be produced in the neutrino burst during type II supernovae in the so-called ν-process by the ^{180}Hf(ν,e^{-})^{180}Ta reaction (Hayakawa et al., 2010). Alternatively, in the same astrophysical site the classical p- or γ-process may produce some ^{180}Ta by photodestruction of ^{181}Ta in the ^{181}Ta(γ,n)^{180}Ta reaction (Arnould & Goriely 2003; Utsunomiya et al., 2006). Similar conditions for the temperature of several billions Kelvin (or $kT ≈ 200 – 300$ keV) occur in type Ia supernovae, and it has been found that some ^{180}Ta can also be made in that site (Travaglio et al., 2011). In addition, some ^{180}Ta may also be produced in the s-process via β-decay of thermally excited ^{179}Hf to ^{179}Ta and subsequent neutron capture in the ^{179}Ta(n,γ)^{180}Ta reaction or via isomeric β-decay of ^{180m}Hf in the

[179]Hf(n,γ)[180m]Hf(β-)[180m]Ta reaction chain (Schumann & Käppeler, 1999; Beer & Ward, 1981; Yokoi & Takahashi, 1983; Mohr et al., 2007).

A common problem in all above production scenarios is the survival of [180]Ta in its isomeric state. If the production occurs in a high-temperature environment like any supernova explosion, then [180]Ta is produced in thermal equilibrium between the low-*K* ground state band and the high-*K* isomeric band. Following the evolution of the isomer-to-ground state ratio, freeze-out is found around 40 keV with a survival probability of [180]Ta in its isomeric state of 0.38±0.01 (Hayakawa et al., 2010). Under s-process conditions with its lower temperature, it is not clear how much [180]Ta can survive in the isomeric state because of mixing between hotter and cooler areas of the thermally pulsing AGB star (Mohr et al., 2007). The resulting yield of [180]Ta depends sensitively on the properties of the lowest intermediate state (IMS) which couples the low-*K* and high-*K* bands.

There is indirect confirmation for the existence of IMS which couple the low-*K* ground state and the high-*K* isomeric state from photoactivation experiments (Belic et al., 2002; Collins et al., 1990). However, no direct γ-transition has been observed up to now. Based on reasonable estimates for transition strengths it has been suggested (Mohr et al., 2007) that the lowest IMS is located at an excitation energy of 594 keV with *J*=(5). This state decays with a transition energy of 72 keV and a half-life of about 16 ns to the low-*K* side of [180]Ta. A weak branch to the high-K side can be expected via a transition to the 7[+] state at 357 keV. This may lead to thermalization of [180]Ta within days at the s-process temperatures around 25 keV (Mohr et al., 2007).

Because of the low transition energy of only 72 keV, a significant modification of the corresponding transition strength can be expected. Enhancements of the radiative strength of up to a factor of 10 for this transition have been calculated (Gosselin et al., 2010) which are mainly based on NEEC. However, unfortunately the influence on the stellar transition rate between low-*K* states and high-*K* states remains very small. The stellar transition rate as given in Eq. (12) is essentially defined by the weak branch of the 594 keV state which has a transition energy of more than 200 keV. As transitions with such high energies are practically not affected by the plasma environment, the stellar transition rate remains almost unchanged.

4.3 [8]B, the [7]Be(p,γ)[8]B reaction, and solar neutrino production

The [7]Be(p,γ)[8]B reaction is the key reaction for the production of high-energy neutrinos in our sun. It is one of the very few examples for a capture reaction between light nuclei where low-energy γ-rays play a significant role. The Q-value of this reaction is extremely low (137 keV), and together with the most effective energy of about 18 keV (at temperatures around 15 million Kelvin, typical for the center of our sun) we find a transition energy of about 155 keV in the low-mass (*Z*=5) nucleus [8]B. The γ-energy of 155 keV is still too high to be significantly influenced by the surrounding plasma. Although experimental conditions in the laboratory (either a proton beam and neutral [7]Be target or a [7]Be beam in arbitrary charge state on a neutral hydrogen target) are quite different from the stellar environment of [7]Be, the cross sections from laboratory experiments do not require a plasma correction for the electromagnetic transition strength to calculate the stellar reaction rates, as e.g. summarized in the NACRE compilation (Angulo et al., 1999)

or in a compilation of solar fusion cross sections (Adelberger et al., 2011). However, two further effects of the surrounding plasma have to be kept in mind here: (i) The electron capture decay of ^{7}Be is significantly affected under solar conditions because electrons have to be captured from the surrounding plasma instead of the bound K-shell electrons for ^{7}Be in a neutral beryllium atom. (ii) Electron screening affects all capture cross sections at very low energies. Because the electronic environment is different in laboratory experiments and under stellar conditions, different corrections have to be applied here.

5. Conclusion

The description of nuclear excitation in hot astrophysical plasma environment requires an accurate knowledge of each individual excitation process. The dominant processes are photo-excitation, where a photon close to the resonant nuclear transition energy is absorbed by the nucleus, NEEC and NEET, where an electron from the continuum (NEEC) or an outer electronic shell (NEET) is captured in a vacancy of the electronic cloud, and inelastic electron scattering, where an incident electron gives a part of its energy to excite the nucleus.

Results for the excitation of the first isomeric state of ^{171}Tm clearly exhibit a strong dependence upon the plasma temperature. The nuclear lifetime under plasma conditions is more than one order of magnitude higher than the laboratory value. All these calculations are made at Local Thermodynamic Equilibrium (LTE), a condition encountered in many astrophysical plasmas.

However, nuclear excitation models in plasma need to be elaborated further. NEET rates require to take into account detailed electronic configuration, as the mean RAAM configuration is more often than not far from a real configuration on which NEET can occur. For high density plasmas, electron inelastic scattering is a major process and screening effects will have to be added to the description.

In most astrophysical scenarios the influence of the surrounding plasma on astrophysical reaction rates will remain relatively small because the γ-transition energies are too high to be significantly affected by the electronic environment. Note that typical γ-transition energies exceed by far 1 MeV whereas plasma effects become most important below 100 keV. Nevertheless, it should be always kept in mind that γ-transitions with energies below about 100 keV may be modified dramatically. As soon as such a transition defines the stellar transition rate, the calculated stellar reaction rate without consideration of plasma effects may be wrong; this error may reach one order of magnitude in special cases, i.e. for very low γ-transition energies.

Such cases with small γ-transition energies (and thus huge influence of the plasma environment) can be found in particular in the astrophysical s-process where the production and destruction of so-called K-isomers proceeds by low-energy γ-transitions which connect the low-K and high-K parts of the excitation spectrum of heavy nuclei via intermediate states. However, for the two most prominent examples (^{176}Lu and ^{180}Ta) it is found that plasma effects remain relatively small for the resulting stellar reaction rates although one particular transition in ^{180}Ta is enhanced by about a factor of 10.

## 6. Acknowledgments

7. References

Abdallah, J. & Sherrill, M.E. (2008). *High Energy Density Physics,* Vol 83, pp 195-245

Adelberger, E. G.; et al. (2011). *Review of Modern Physics,* Vol 83, pp 195-245

Alder, K.; Bohr, A.; Huus, T.; Mottelson, B.; & Winther, A. (1956). *Review of Modern Physics*, Vol 28 pp 432-542

Angulo, C.; et al. (1999). *Nuclear Physics A,* Vol 656, pp 3-187

Arnould, M. & Goriely, S. (2003). *Physics Reports,* Vol 384, pp 1-84

Arnould, M. & Goriely, S. (2012). The r-process of nucleosynthesis: The puzzle is still with us, In: *Nucleosynthesis*, InTech, 978-953-308-32-9, Rijeka, Croatia.

Baglin, C. M. (2002). *Nuclear Data Sheets*, Vol 96, pp 399-610; available online at *http://www.nndc.bnl.gov/ensdf.*

Basunia, M. S. (2006). *Nuclear Data Sheets,* Vol 107, pp 791-1026; available online at *http://www.nndc.bnl.gov/ensdf*

Beer, H. & Ward, R. A. (1981). *Nature,* Vol 291, pp 308-310

Belic, D.; et al. (2002). *Physical Review C,* Vol 65, pp 035801

Bosch, F.; et al. (1996). *Physical Review Letters,* Vol 77, pp 5190-5193

Collins, C. B.; et al. (1990). *Physical Review C,* Vol 42, pp R1813-R1816

Doll, C.; et al. (1999). *Physical Review C,* Vol 59, pp 492-499

Doolen, G. D. (1978). *Physical Review C,* Vol 18, pp 2547-2559

Dracoulis, G. D.; et al. (2010). *Physical Review C,* Vol 81, pp 011301(R)

Farkas, J.; et al. (2009). *Journal of Physics G,* Vol 36, pp 105101

Faussurier, G.; Blancard, C. & Decoster, A. (1997). *Physical Review E,* Vol 56, pp 3474

Gallino, R.; et al. (1998). *Astrophysical Journal,* Vol 497, pp 388-403

Gintautas, V.; Champagne, A. E.; Kondev, F. G. & Longland, R. (2009). *Physical Review C,* Vol 80, pp 015806

Gosselin, G.; Méot, V. & Morel, P. (2007). *Physical Review C,* Vol 76, pp 044611

Gosselin, G. & Morel, P. (2004). *Physical Review C,* Vol 70, pp 064603

Gosselin, G.; Morel, P. & Mohr, P. (2010). *Physical Review C,* Vol 81, pp 055808

Gosselin, G.; Pillet, N.; Méot, V.; Morel, P. & Dzyublik, A. Ya. (2009). *Physical Review C,* Vol 79, pp 014604

Hamilton, W. D. (1975). *The Electromagnetic Interaction in Nuclear Spectroscopy,* Elsevier, ISBN 0 444 10519 O, New York, USA

Hayakawa, T.; Mohr, P.; Kajino, T.; Chiba, S. & Mathews, G. J. (2010). *Physical Review C,* Vol 82, pp 055801

Heil, M.; et al. (2008). *Astrophysical Journal,* Vol 673, pp 434-444

Hult, M.; Gasparro, J.; Marissens, G.; Lindahl, P.; Wäthjen, U.; Johnston, P. & Wagemans, C. (2006). *Physical Review C,* Vol 74, pp 054311

Iliadis, C. (2007). *Nuclear Physics of Stars*, Wiley-VCH, 978-3-527-40602-9, Weinheim, Germany.

Käppeler, F.; Gallino, R.; Bisterzo, S. & Aoki, W. (2011). *Review of Modern Physics,* Vol 83, pp 157-193

Kimball, J. C.; Bittel, D. & Cue, N. (1991). *Physics Letters A,* Vol 152, pp 367-370

Klay, N.; et al. (1991). *Physical Review C,* Vol 44, pp 2801-2838

Kücük, I. (2012). Screening Factors and Thermonuclear Reaction Rates for Low Mass Stars, In: *Nucleosynthesis*, InTech, 978-953-308-32-9, Rijeka, Croatia.

Lesko, K. T.; et al. (1991). *Physical Review C,* Vol 44, pp 2850-2864

Lodders, K. (2003). *Astrophysical Journal,* Vol 591, pp 1220-1247

Marss, R. (2010), *XI'th International Symposium on EBIS and EBIT*, *7-10 April 2010,* UCRL-PRES-427008, Livermore, California, USA

Matteucci, F. (2012). Stellar Nucleosynthesis, In: *Nucleosynthesis*, InTech, 978-953-308-32-9, Rijeka, Croatia.

Messiah, A. (1961). *Quantum Mechanics,* North Holland, ISBN 0 471 59766 X, Amsterdam, Holland

Mohr, P.; Käppeler, F. & Gallino, R. (2007). *Physical Review C,* Vol 75, pp 012802(R)

Mohr, P.; Fülöp, Zs. & Utsunomiya, H. (2007b). *European Physical Journal A,* Vol 32, pp 357-369

Mohr, P.; Bisterzo, S.; Gallino, R.; Käppeler, F.; Kneissl, U. & Winckler, N. (2009). *Physical Review C,* Vol 79, pp 045804

Morel, P.; Méot, V.; Gosselin, G.; Gogny, D. & Yunnes, W. (2004). *Physical Review A,* Vol 69, pp 063414

Ohtsuki, T.; Yuki, H.; Muto, M.; Kasagi, J. & Ohno, K. (2004). *Physical Review Letters,* Vol 93, pp 112501

Pumo, M. L. (2012). The s-process nucleosynthesis in massive stars: current status and uncertainties due to convective overshooting, In: *Nucleosynthesis*, InTech, 978-953-308-32-9, Rijeka, Croatia.

Rauscher, T.; Mohr, P.; Dillmann, I. & Plag, R. (2011). *Astrophysical Journal,* Vol 738, pp 143

Rolfs, C. E. & Rodney, W. S. (1988). *Cauldrons in the Cosmos*, The University of Chicago Press, 0-226-72456-5, Chicago, IL, USA.

Rozsnyai, B. F. (1972). *Physical Review A,* Vol 5, pp 1137-1149

Schumann, M. & Käppeler, F. (1999). *Physical Review C,* Vol 60, pp 025802

Takahashi, K. & Yokoi, K. (1987). *Atomic Data Nuclear Data Tables,* Vol 36, pp 375-409

Travaglio, C.; Roepke, F.; Gallino, R. & Hillebrandt, W. (2011). *Astrophysical Journal,* Vol 739, pp 93

Utsunomiya, H.; Mohr, P.; Zilges, A. & Rayet, M. (2006). *Nuclear Physics A,* Vol 777, pp 459-478

Ward, R. A. & Fowler, W. A. (1980). *Astrophysical Journal,* Vol 238, pp 266-286

Wu, S. C. & Niu, H. (2003). *Nuclear Data Sheets,* Vol 100, pp 483-705; available online at *http://www.nndc.bnl.gov/ensdf*

Yokoi, K. & Takahashi, K. (1983). *Nature,* Vol 305, pp 198-200
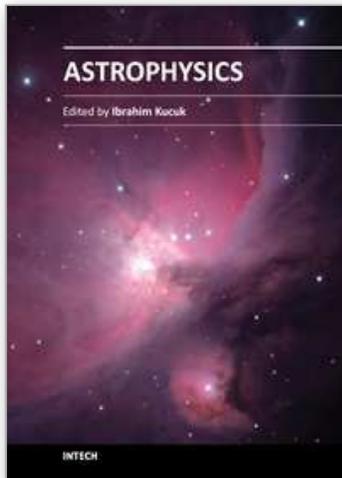
Astrophysics

Edited by Prof. Ibrahim Kucuk

This book provides readers with a clear progress to theoretical and observational astrophysics. It is not surprising that astrophysics is continually growing because very sophisticated telescopes are being developed and they bring the universe closer and make it accessible. Astrophysics Book presents a unique opportunity for readers to demonstrate processes do occur in Nature. The unique feature of this book is to cover different aspects in astrophysics covering the topics: • Astronomy • Theoretical Astrophysics • Observational Astrophysics • Cosmology • The Solar System • Stars • Planets • Galaxies • Observation • Spectroscopy • Dark Matter • Neutron Stars • High Energy Astrophysics

How to reference

In order to correctly reference this scholarly work, feel free to copy and paste the following:

G. Gosselin, P. Mohr, V. Méot and P. Morel (2012). Nuclear Excitation Processes in Astrophysical Plasmas, Astrophysics, Prof. Ibrahim Kucuk (Ed.), ISBN: 978-953-51-0473-5, InTech, Available from: http://www.intechopen.com/books/astrophysics/nuclear-excitation-processes-in-astrophysical-plasmas

INTECH
open science | open minds